

Longitudinal and Transverse Zeeman Ladders in the Ising-Like Chain Antiferromagnet $\text{BaCo}_2\text{V}_2\text{O}_8$

B. Grenier,^{1,2,*} S. Petit,³ V. Simonet,^{4,5} E. Canévet,⁶ L.-P. Regnault,^{1,2} S. Raymond,^{1,2} B. Canals,^{4,5}
C. Berthier,^{7,8} and P. Lejay^{4,5}

¹Université Grenoble Alpes, INAC-SPSMS, F-38000 Grenoble, France

²CEA, INAC-SPSMS, F-38000 Grenoble, France

³Laboratoire Léon Brillouin, CEA-CNRS, CEA-Saclay, F-91191 Gif-sur-Yvette, France

⁴CNRS, Institut Néel, F-38042 Grenoble, France

⁵Université Grenoble Alpes, Institut Néel, F-38042 Grenoble, France

⁶Institut Laue-Langevin, CS 20156, F-38042 Grenoble Cedex 9, France

⁷Université Grenoble Alpes, Laboratoire National des Champs Magnétiques Intenses, F-38000 Grenoble, France

⁸CNRS, Laboratoire National des Champs Magnétiques Intenses, F-38000 Grenoble, France

(Received 24 June 2014; published 6 January 2015)

We explore the spin dynamics emerging from the Néel phase of the chain compound antiferromagnet $\text{BaCo}_2\text{V}_2\text{O}_8$. Our inelastic neutron scattering study reveals unconventional discrete spin excitations, so-called Zeeman ladders, understood in terms of spinon confinement, due to the interchain attractive linear potential. These excitations consist of two interlaced series of modes, respectively, with transverse and longitudinal polarization. The latter, which correspond to a longitudinal fluctuation of the ordered moment, have no classical counterpart and are related to the zero-point fluctuations that weaken the ordered moment in weakly coupled quantum chains. Our analysis reveals that $\text{BaCo}_2\text{V}_2\text{O}_8$, with moderate Ising anisotropy and sizable interchain interactions, remarkably fulfills the conditions necessary for the observation of discrete long-lived longitudinal excitations.

DOI: [10.1103/PhysRevLett.114.017201](https://doi.org/10.1103/PhysRevLett.114.017201)

PACS numbers: 75.10.Pq, 75.30.Ds, 75.50.Ee, 78.70.Nx

The nature of the excitations in spin half antiferromagnets is a topic of considerable current interest in the field of quantum magnetism. The one-dimensional (1D) case is especially interesting as quantum fluctuations melt the classical long-range Néel order. The ground state remains disordered, with a spin excitation spectrum consisting of a continuum composed of pairs of $S = 1/2$ excitations called spinons, created or destroyed in pairs, like domain walls in an Ising magnet. Physical realizations of 1D systems, however, eventually order at very low temperature, owing to a small coupling between chains. The metamorphosis of the continuum of spinons that accompany this dimensional crossover towards a 3D state is an appealing issue [1].

The three possible spin states $S = \pm 1, 0$ for a pair of spinons transform upon ordering into two transverse modes and a third collective excitation, which corresponds to fluctuations parallel to the direction of the ordered moment, hence a *longitudinal* mode. The observation of the latter is a key issue in condensed matter studies, especially in magnetism with the case of Heisenberg quantum antiferromagnets [2–4], and beyond: If a continuous symmetry is broken, transverse and longitudinal modes are expected in the ordered phase, identified as Goldstone and amplitude modes, respectively [5,6]. The latter is the analog of what is known in particle theory literature as the Higgs particle [4]. Its detection is challenging, since it is generally overdamped because of its decay into massless transverse excitations.

In parallel, another peculiarity of the 1D to 3D dimensional crossover is that, in the ordered state of quasi-1D systems, each chain experiences an effective staggered molecular field, which gives rise to a linear attractive potential between spinons. The latter competes with their propagating character and finally leads to their confinement in bound states. A spectacular manifestation of this effect in the case of Ising spins, initially described by Shiba [7], is the quantization of the transverse excitation continuum in a series of discrete lines below the Néel temperature (T_N). This effect, called Zeeman ladder, was proposed to explain the discretization of the excitations observed in the ordered phase of CsCoCl_3 and CsCoBr_3 with Raman spectroscopy [7,8]. Recently, a similar series of modes was also observed in the Ising ferromagnetic chain compound CoNb_2O_6 [9,10].

In this Letter, we introduce a new focus on this physics. We examine the excitations of $\text{BaCo}_2\text{V}_2\text{O}_8$, which realizes an XXZ quasi-1D spin $\frac{1}{2}$ antiferromagnet, intermediate between the Ising and Heisenberg cases. By means of inelastic neutron scattering, we describe below T_N the emergence of *long-lived transverse and longitudinal* excitations, in the form of two well-defined *Zeeman ladders*. The exceptional stability of the longitudinal modes is discussed in connection with the presence of discretized transverse excitations gapped by the Ising-like anisotropy [5,6].

$\text{BaCo}_2\text{V}_2\text{O}_8$ consists of screw chains of Co^{2+} running along the fourfold \mathbf{c} axis of the body-centered tetragonal

structure [11]. These chains are weakly coupled, yielding an antiferromagnetic (AF) ordering (propagation vector $\mathbf{k}_{\text{AF}} = (1, 0, 0)$ [12–14]) in zero field below $T_N \approx 5.5$ K [17,18]. The magnetic moment in the distorted octahedral environment is described by a highly anisotropic effective spin $S = 1/2$ [19] with $g_{xy} = 2.95$ and $g_z = 6.2$ [20], thus allowing quantum fluctuations [21]. The validity of this description is sustained by the observation of the first crystal field level at 30 meV [14]. This physics is described by the XXZ Hamiltonian:

$$\mathcal{H} = J \sum_i [\epsilon(S_i^x S_{i+1}^x + S_i^y S_{i+1}^y) + S_i^z S_{i+1}^z], \quad (1)$$

where, according to the analysis of the magnetization curve [21], the intrachain AF interaction is $J = 5.6$ meV and the anisotropy parameter is $\epsilon = 0.46$.

The neutron experiment was performed on the JCNS/CEA–CRG cold neutron three-axis spectrometer IN12 at the Institut Laue-Langevin. A series of energy scans at constant scattering vector \mathbf{Q} was measured in the Néel phase to obtain the spin dispersion parallel and perpendicular to the chains.

Direct evidence for the emergence in the ordered phase of unconventional dispersive excitations is shown in Fig. 1. At the zone center $\mathbf{Q} = (2, 0, 2)$, a series of gapped sharp modes ranging between about 1.5 and 6 meV, with decreasing intensities as the energy increases, is observed [see Fig. 1(b)]. These modes show a sizable dispersion along the chain direction [see Fig. 1(a)]. The presence of an intense peak with an out-of-phase weaker dispersion along the \mathbf{c} axis can also be noticed around 6–7 meV. As expected for magnetic excitations, all these modes disappear above T_N [see Fig. 1(b)]. The relative \mathbf{Q} dependence of their intensities and their energy suggest that the peak around 7 meV can be interpreted as an optical mode, whereas the series of low energy excitations is acousticlike. The existence of both types of excitations is indeed expected considering the 16 Co^{2+} ions per unit cell in a classical picture. Yet, this intense mode could alternatively be attributed to a kinetic bound state of spinons or bound state of pairs of spinons [9,10].

In the following, however, we shall focus on the low energy series, and first investigate their polarization. A neutron scattering experiment is only sensitive to the spin components perpendicular to \mathbf{Q} . Since the ordered moment is along the \mathbf{c} axis, measurements with $\mathbf{Q} \parallel \mathbf{c}$ reveal transverse excitations ($\parallel \mathbf{a}$ and $\parallel \mathbf{b}$) while measurements with $\mathbf{Q} \parallel \mathbf{a}$ disclose the superposition of transverse ($\parallel \mathbf{b}$) and longitudinal ($\parallel \mathbf{c}$) excitations. Energy scans were thus measured at $T = 1.6$ K at various \mathbf{Q} positions (see Fig. 2). For $\mathbf{Q} = (0, 0, 2)$, a single series is observed. As the scattering vector rotates towards the \mathbf{a} direction, a twin series of modes, shifted at slightly higher energies, rises progressively with an intensity that increases with respect

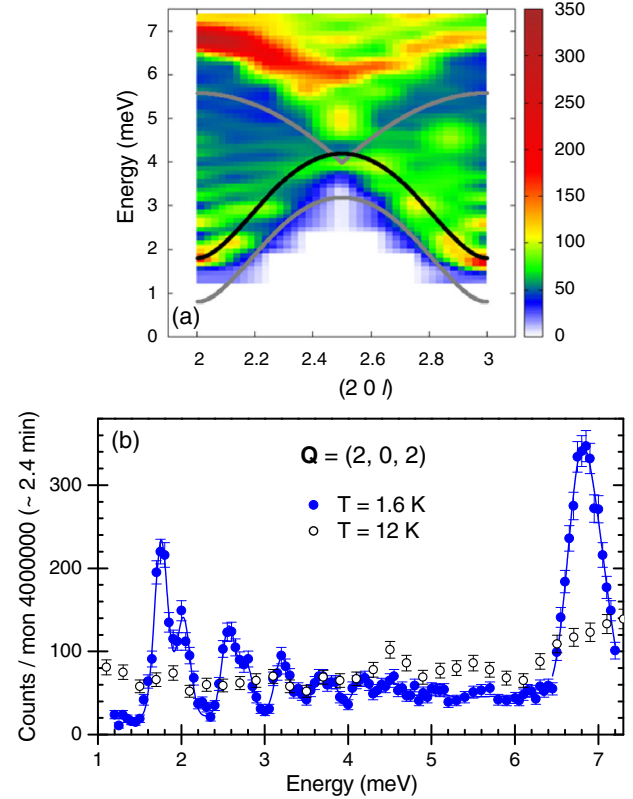


FIG. 1 (color online). (a) Inelastic scattering intensity map obtained from a series of \mathbf{Q} -constant energy scans measured at $T = 1.6$ K. The black line is a fit of the lowest mode of the series E_1^T based on the assumption that its dispersion follows the lower boundary $2E_0^T$ of the two spinon continuum in the purely 1D case (see text). The gray lines indicate the lower and upper boundaries of the corresponding continuum using the fitted $\epsilon = 0.41$ and $J = 2.3$ meV parameters [22]. (b) Energy scans measured at $\mathbf{Q} = (2, 0, 2)$ below and above the Néel temperature.

to the first series. These results prove unambiguously the transverse (T) nature of the first series of discrete modes and the longitudinal (L) nature of the second one.

An important characteristic of this quasi-1D chain system is the strength of the interchain interactions. It can be evidenced from the dispersion of the excitations perpendicular to the chain axis. Figure 3(c) presents the energy dependence of the lowest energy mode of the T and L series along \mathbf{a}^* obtained from the energy scans shown in Figs. 3(a) and 3(b). Although not visible for $l = 1$, a sizable dispersion, of the order of 0.1 meV, is observed for $l = 2$ with an expected minimum of the gapped mode at the AF points. This peculiar l dependence suggests that the coupling of Co spins belonging to adjacent chains and shifted by $c/2$ should be taken into account, while another exchange interaction in the diagonal direction finally stabilizes the observed magnetic structure [14,23].

Next, we extracted the position of the modes in order to investigate the bounding mechanism of the spinons. The modes at $\mathbf{Q} = (0, 0, 2)$ and $\mathbf{Q} = (3, 0, 1)$ were fitted up to

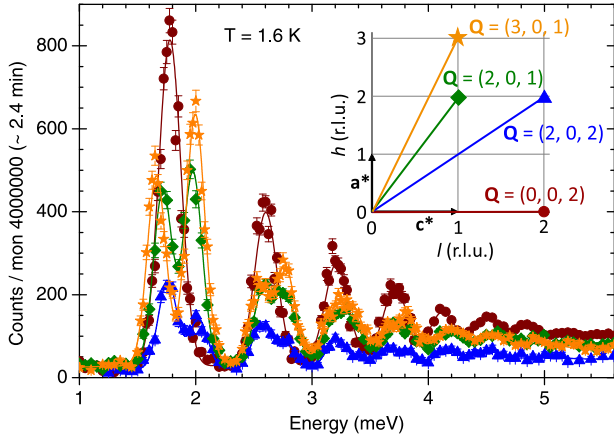


FIG. 2 (color online). \mathbf{Q} -constant energy scans, at various Bragg positions shown in the inset (solid symbols), fitted by a series of Gaussian functions (solid lines). This figure emphasizes two series of interlaced sharp T and L modes, the latter arising and increasing in intensity when the \mathbf{Q} vector rotates from the c axis towards the \mathbf{a} axis direction.

6 meV by a series of Gaussian functions (see Fig. 4). Their full width at half maximum was obtained from a fit of the lowest energy T and L modes and held constant to the same value (0.2 meV) for the subsequent modes of the series.

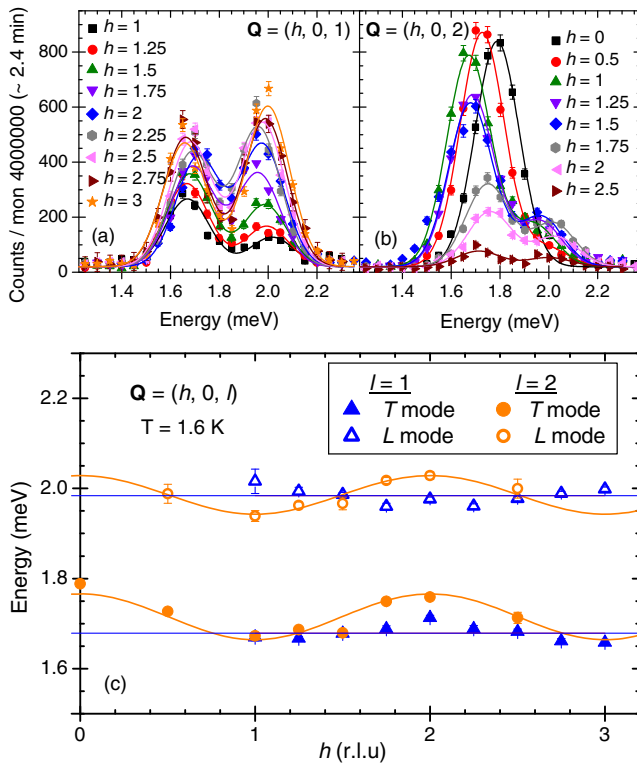


FIG. 3 (color online). \mathbf{Q} -constant energy scans measured at 1.6 K (solid symbols) for (a) $\mathbf{Q} = (h, 0, 1)$ and (b) $\mathbf{Q} = (h, 0, 2)$ scanning the lowest T and L modes of the series. These modes are fitted by two Gaussian functions (solid lines), yielding their dispersion curves along \mathbf{a}^* plotted in panel (c). The solid lines are a guide for the eyes.

It was necessary to add an increasing background as the energy increases, probably due to a continuum of excitations. For $\mathbf{Q} = (0, 0, 2)$, eight sharp T modes could be extracted. For $\mathbf{Q} = (3, 0, 1)$, five T modes and five L modes could be separated. The sixth and seventh modes of the series were fitted by a unique Gaussian function including the T and L modes too close in energy to be separated. This analysis shows that the spacing between the modes appears in a very nontrivial sequencing.

In order to interpret these results, a good starting point is the pure 1D quasi-Ising limit [$\epsilon \ll 1$ in Eq. (1)]. A state containing two spinons is created by reversing one or several adjacent spins from one of the two degenerate Néel states. Two AF bonds are broken, yielding a state with energy J , degenerate with all states resulting from reversing an arbitrary number of subsequent spins. These states carry a spin $S_z = \pm 1$ for an odd number of reversed spins and $S_z = 0$ for an even number. As soon as $\epsilon \neq 0$, the excitation spectrum becomes a continuum composed of such two domain walls which propagate independently. In this picture, the $S_z = \pm 1$ states form transverse excitations, while the $S_z = 0$ states form longitudinal ones. This 1D domain wall picture and the existence of a gapped continuum were first described by Villain [24]. Shiba then

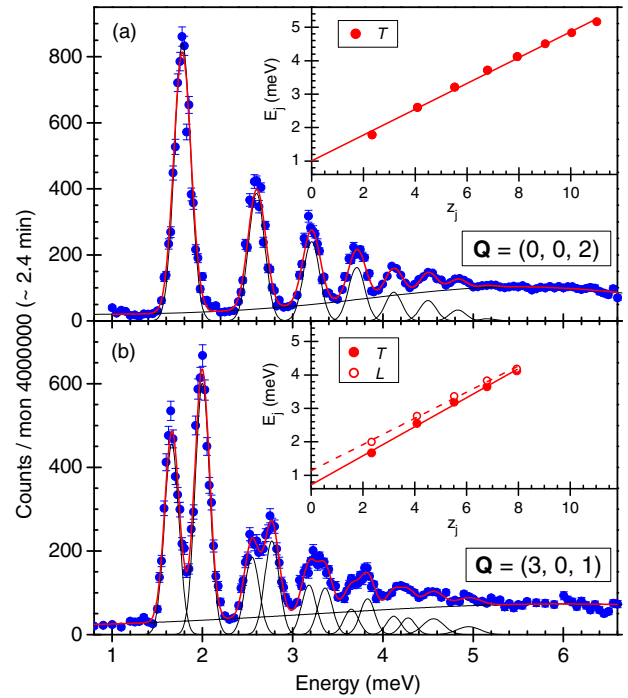


FIG. 4 (color online). Energy scans measured (solid symbols) for (a) $\mathbf{Q} = (0, 0, 2)$ and (b) $\mathbf{Q} = (3, 0, 1)$. These series of sharp modes, as well as a broad contribution, were fitted by Gaussian functions (red line for the global fit and black lines for the individual Gaussian functions, see text). The energies of the excitations extracted from the fits are plotted in the insets as a function of the negative zeros z_l of the Airy function (see text). The lines are linear fits to the data.

showed that the introduction of interchain couplings J' , acting as a molecular field h_m , gives to the two domain wall states an additional potential energy proportional to the distance between them. This causes the above mentioned quantization of the excitation continuum which appears as a series of discrete dispersing lines below the 3D ordering temperature [7–9,21].

The linear form of the confining potential imposes that the sequence of excited modes should follow the negative zeros of the Airy function Ai [9,25–27]. We thus analyze, at the bound state dispersion minima, the sequence of their energies with

$$E_j^{T,L} = 2E_0^{T,L} + \alpha z_j \quad \text{with } j = 1, 2, 3, \dots, \quad (2)$$

with $\text{Ai}(-z_j) = 0$ and $\alpha \approx (h_m^2 \epsilon J)^{1/3}$ [9]. As shown in the insets of Fig. 4, the energies of the T and L modes were satisfactorily fitted to Eq. (2) for various \mathbf{Q} , validating the spinon confinement mechanism. The fit yielded $\alpha \approx 0.42 \pm 0.03$ meV, $2E_0^T \approx 0.85 \pm 0.15$ meV, and $2E_0^L \approx 1.08 \pm 0.05$ meV [14]. In the absence of any microscopic model taking into account both arbitrary ϵ and interchain interaction (Shiba's model is valid only for $\epsilon \ll 1$), we then assume that the dispersion along \mathbf{c}^* of the first bound state E_1^T is roughly similar to that of the lower boundary of the two-spinon continuum in the pure 1D case, namely $2E_0^T$. For any J and ϵ , this boundary is given by [22]:

$$2E_0^T(l) = \begin{cases} \frac{2J}{1+\kappa} \sqrt{1 + \kappa^2 - 2\kappa \cos \pi l} & \text{for } l \leq \ell_\kappa \\ \frac{2J}{1+\kappa} \sin \pi l & \text{for } \ell_\kappa \leq l \leq 1 - \ell_\kappa \\ \frac{2J}{1+\kappa} \sqrt{1 + \kappa^2 + 2\kappa \cos \pi l} & \text{for } l \geq 1 - \ell_\kappa, \end{cases} \quad (3)$$

with $\cos(\pi \ell_\kappa) = \kappa$, $k' = (1 - \kappa/1 + \kappa)$, $k = \sqrt{1 - k'^2}$, $1/\epsilon = \cosh(\pi K'/K)$, and $J = I\pi/[K \tanh(\pi K'/K)]$ (K and K' are the elliptic integrals of argument k and k' , respectively) [28].

Fitting the dispersion along \mathbf{c}^* of $E_1^T - \alpha z_1 = 2E_0^T(l)$ with this model in several Brillouin zones gives $J \approx 2.8 \pm 0.4$ meV and $\epsilon \approx 0.41 \pm 0.02$ (see, e.g., Fig. 1). This analysis locates $\text{BaCo}_2\text{V}_2\text{O}_8$ in the intermediate anisotropic regime, in agreement with previous estimations of ϵ [21,29]. Note that J is twice smaller than the estimation given in Refs. [20,21]. Last, h_m is directly proportional to an effective interchain interaction J'_{eff} . A quite strong value of $h_m \sim 0.3$ meV $\propto J'_{\text{eff}}$ can be inferred from the determination of α . This somewhat larger value than the ~ 0.1 meV amplitude of the dispersion along \mathbf{a}^* is probably due to the frustration between the various interchain couplings [14].

It is worth noting that in the $\epsilon \ll 1$ limit, the distinguishing feature of the L excitations is the existence of a specific coupling with the Néel states. As the ϵ term exchanges two neighboring spins, the Néel state is directly coupled to

$S_z = 0$ excited states containing two reversed spins. This makes the longitudinal modes more massive (at higher energy) than their transverse counterpart, as we observe in $\text{BaCo}_2\text{V}_2\text{O}_8$. The ground state is then an admixture of $S_z = 0$ two domain wall states added to the Néel state, producing a weakening of the ordered moment. In the $\epsilon \ll 1$ limit, the intensity of the L modes should scale with ϵ^2 [8], explaining why L excitations were hardly observed in systems close to the Ising limit such as CsCoCl_3 and CsCoBr_3 [7,30]. The somehow more isotropic character of $\text{BaCo}_2\text{V}_2\text{O}_8$ (larger ϵ value), however, is expected to enhance the L modes.

In the limit of purely isotropic Heisenberg spins ($\epsilon = 1$), a longitudinal mode is also expected [6]. It was, for instance, observed as a damped excitation, in the antiferromagnetically ordered phases of spin $\frac{1}{2}$ dimer system TlCuCl_3 [4], close to the pressure-induced ordering transition, and of quasi-1D Heisenberg spin $\frac{1}{2}$ antiferromagnet KCuF_3 [31]. The longitudinal mode damping is usually attributed to its decay into a pair of gapless transverse spin waves. This longitudinal mode could, however, not be resolved in another 1D material, namely $\text{BaCu}_2\text{Si}_2\text{O}_7$, which has a much weaker interchain coupling [32]. A sufficiently strong dispersion perpendicular to the chains was suggested to be necessary in order to additionally stabilize such a damped longitudinal mode. In $\text{BaCo}_2\text{V}_2\text{O}_8$, we have indeed determined sizable interchain couplings. Moreover, in contrast to the experimental observation in KCuF_3 , the $\text{BaCo}_2\text{V}_2\text{O}_8$ longitudinal modes are remarkably intense and resolution limited. The reason is probably that these longitudinal modes cannot decay into transverse modes since the latter have a large gap, due to the Ising-like anisotropy, and are discretized. It is worth noting that this discretization of longitudinal modes has been reported for the Higgs modes in optical lattice of cold atoms due to confinement [3].

It is finally very instructive to recall that $\text{BaCo}_2\text{V}_2\text{O}_8$ has also raised recently much interest for its field-induced behavior, describable in terms of Tomonaga-Luttinger liquid physics [12,13,33]. An exotic magnetic ordered phase, unknown in classical systems, is induced by a magnetic field applied parallel to the chain axis. A longitudinal incommensurate spin density wave (amplitude of the moments modulated along the field direction) is actually stabilized thanks to the particular values of J' and ϵ [29]. Those ingredients, i.e., sizable interchain interactions and intermediate anisotropic character, are the same as the ones we have invoked to account for the quantized transverse and longitudinal magnetic excitations, observed in $\text{BaCo}_2\text{V}_2\text{O}_8$. This material is thus a rare example of a spin $1/2$ system displaying spin longitudinal modes, of pure quantum origin, in both the dynamical and the field-induced static regimes.

To summarize, our inelastic neutron scattering experiment has revealed unconventional spin excitations in the

Ising-like chain antiferromagnet $\text{BaCo}_2\text{V}_2\text{O}_8$: They are quantized due to a weak interchain coupling and consist of two interlaced series of transverse and remarkably strong longitudinal Zeeman ladders. We propose that the stabilization of these longitudinal modes is enabled by the moderate Ising anisotropy prohibiting their decay into the gapped and discretized transverse modes.

We would like to thank R. Ballou, J. Robert, and T. Ziman for fruitful discussions and B. Vettard for his technical support. This work was partly supported by the French ANR Project NEMSICOM.

*Corresponding author.
grenier@ill.fr

- [1] A. Zheludev, *Appl. Phys. A* **74**, s1 (2002).
- [2] D. Podolsky, A. Auerbach, and D. P. Arovas, *Phys. Rev. B* **84**, 174522 (2011).
- [3] M. Endres, T. Fukuhara, D. Pekker, P. Schauss, C. Gross, E. Demler, S. Kuhr, and I. Bloch, *Nature (London)* **487**, 454 (2012).
- [4] Ch. Rüegg, B. Normand, M. Matsumoto, A. Furrer, D. F. McMorrow, K. W. Krämer, H.-U. Güdel, S. N. Gvasaliya, H. Mutka, and M. Boehm, *Phys. Rev. Lett.* **100**, 205701 (2008); P. Merchant, B. Normand, K. W. Krämer, M. Boehm, D. F. McMorrow, and Ch. Rüegg, *Nat. Phys.* **10**, 373 (2014).
- [5] I. Affleck and G. F. Wellman, *Phys. Rev. B* **46**, 8934 (1992).
- [6] H. J. Schulz, *Phys. Rev. Lett.* **77**, 2790 (1996).
- [7] H. Shiba, *Prog. Theor. Phys.* **64**, 466 (1980).
- [8] N. Ishimura and H. Shiba, *Prog. Theor. Phys.* **63**, 743 (1980).
- [9] R. Coldea, D. A. Tennant, E. M. Wheeler, E. Wawrzynska, D. Prabhakaran, M. Telling, K. Habicht, P. Smeibidl, and K. Kiefer, *Science* **327**, 177 (2010).
- [10] C. M. Morris, R. Valdés Aguilar, A. Ghosh, S. M. Koohpayeh, J. Krizan, R. J. Cava, O. Tchernyshyov, T. M. McQueen, and N. P. Armitage, *Phys. Rev. Lett.* **112**, 137403 (2014).
- [11] R. Wichmann and Hk. Müller-Buschbaum, *Z. Anorg. Allg. Chem.* **534**, 153 (1986).
- [12] S. Kimura, M. Matsuda, T. Masuda, S. Hondo, K. Kaneko, N. Metoki, M. Hagiwara, T. Takeuchi, K. Okunishi, Z. He, K. Kindo, T. Taniyama, and M. Itoh, *Phys. Rev. Lett.* **101**, 207201 (2008).
- [13] E. Canévet, B. Grenier, M. Klanjšek, C. Berthier, M. Horvatić, V. Simonet, and P. Lejay, *Phys. Rev. B* **87**, 054408 (2013).
- [14] See Supplemental Material at <http://link.aps.org/supplemental/10.1103/PhysRevLett.114.017201> for information on the crystal and magnetic structures and complementary inelastic neutron scattering results, which includes Refs. [15,16].
- [15] P. Lejay, E. Canévet, S. K. Srivastava, B. Grenier, M. Klanjšek, and C. Berthier, *J. Cryst. Growth* **317**, 128 (2011).
- [16] K. Penc, J. Romhányi, T. Rőöm, U. Nagel, Á. Antal, T. Fehér, A. Jánossy, H. Engelkamp, H. Murakawa, Y. Tokura, D. Szaller, S. Bordács, and I. Kézsmárki, *Phys. Rev. Lett.* **108**, 257203 (2012).
- [17] Z. He, D. Fu, T. Kyōmen, T. Taniyama, and M. Itoh, *Chem. Mater.* **17**, 2924 (2005).
- [18] Z. He, T. Taniyama, and M. Itoh, *Appl. Phys. Lett.* **88**, 132504 (2006).
- [19] A. Abragam and M. H. L. Pryce, *Proc. R. Soc. A* **206**, 173 (1951).
- [20] S. Kimura, H. Yashiro, M. Hagiwara, K. Okunishi, K. Kindo, Z. He, T. Taniyama, and M. Itoh, in *Proceedings of the Yamada Conference LX on Research in High Magnetic Fields, Sendai, Japan, 2006* [*J. Phys. Conf. Ser.* **51**, 99 (2006)].
- [21] S. Kimura, H. Yashiro, K. Okunishi, M. Hagiwara, Z. He, K. Kindo, T. Taniyama, and M. Itoh, *Phys. Rev. Lett.* **99**, 087602 (2007).
- [22] A. H. Bougourzi, M. Karbach, and G. Müller, *Phys. Rev. B* **57**, 11429 (1998).
- [23] M. Klanjšek, M. Horvatić, S. Kramer, S. Mukhopadhyay, H. Mayaffre, C. Berthier, E. Canévet, B. Grenier, P. Lejay, and E. Orignac, [arXiv:1412.2411](https://arxiv.org/abs/1412.2411).
- [24] J. Villain, *Physica B+C* **79**, 1 (1975).
- [25] B. M. McCoy and T. T. Wu, *Phys. Rev. D* **18**, 1259 (1978).
- [26] S. T. Carr and A. M. Tselik, *Phys. Rev. Lett.* **90**, 177206 (2003).
- [27] S. B. Rutkevich, *J. Stat. Phys.* **131**, 917 (2008).
- [28] Note that the lower boundary is gapped as soon as $\epsilon < 1$.
- [29] K. Okunishi and T. Suzuki, *Phys. Rev. B* **76**, 224411 (2007).
- [30] A. Oosawa, K. Kakurai, Y. Nishiwaki, and T. Kato, *J. Phys. Soc. Jpn.* **75**, 074719 (2006).
- [31] B. Lake, D. A. Tennant, and S. E. Nagler, *Phys. Rev. Lett.* **85**, 832 (2000).
- [32] A. Zheludev, S. Raymond, L.-P. Regnault, F. H. L. Essler, K. Kakurai, T. Masuda, and K. Uchinokura, *Phys. Rev. B* **67**, 134406 (2003).
- [33] S. Kimura, T. Takeuchi, K. Okunishi, M. Hagiwara, Z. He, K. Kindo, T. Taniyama, and M. Itoh, *Phys. Rev. Lett.* **100**, 057202 (2008).